Research Square

Preprints are preliminary reports that have not undergone peer review.
They should not be considered conclusive, used to inform clinical practice,
or referenced by the media as validated information.

Contribution of Satellite Precipitation Data to Hydrological Modeling in Data-Limited Contexts: A Case Study in Morocco

Imane El Martili

imane.elmartili.cedoc@ehtp.ac.ma

Hassania School of Public Works

Jihane Ahattab

Hassania School of Public Works

Khalid Barkouki

Hassania School of Public Works

Saad Bensallam

Hassania School of Public Works

Research Article

Keywords: PERSIANN-CCS, satellite precipitation, rainfall–runoff modelling, HEC-HMS, hydrological modelling, semi-arid watershed

Posted Date: November 12th, 2026

DOI: https://doi.org/10.21203/rs.3.rs-10796784/v1

License: This work is licensed under a Creative Commons Attribution 4.0 International License.
Read Full License

Additional Declarations: No competing interests reported.

Contribution of Satellite Precipitation Data to Hydrological Modeling in Data-Limited Contexts: A Case Study in Morocco

Abstract

Satellite precipitation products have become an important source of rainfall information for hydrological studies, particularly in regions where ground observations are sparse or incomplete. Evaluating their capability to reproduce watershed hydrological responses is therefore essential before they can be used for flood modelling and water resources applications. This study assesses the performance of the Precipitation Estimation from Remotely Sensed Information using Artificial Neural Networks–Cloud Classification System (PERSIANN-CCS) satellite precipitation product for rainfall–runoff simulation in the Oued Nfifikh watershed (Morocco) using the HEC-HMS rainfall–runoff model. A sensitivity analysis was first carried out to identify the most influential model parameters. The model was then calibrated manually and subsequently optimized through automatic calibration using six flood events, while three independent events were used for validation. To ensure an objective comparison, the same calibrated parameter set was applied to simulations driven by both observed rainfall and PERSIANN-CCS precipitation. Model performance was evaluated using the Nash–Sutcliffe efficiency (NSE), root mean square error (RMSE), mean absolute error (MAE), percent bias (PBIAS), correlation coefficient (R), and coefficient of determination (R^2). The results showed that both rainfall datasets enabled satisfactory streamflow simulations, although their performance varied from one flood event to another. Event-based comparisons indicated that PERSIANN-CCS precipitation produced results comparable to those obtained with observed rainfall and even outperformed ground observations for several events, demonstrating its potential for rainfall–runoff modelling in semi-arid watersheds. These findings highlight the potential of satellite precipitation products as a reliable alternative or complementary source of rainfall information for hydrological modelling, particularly in data-scarce regions, and provide a sound basis for subsequent hydraulic modelling and flood hazard mapping.

Keywords: PERSIANN-CCS; satellite precipitation; rainfall–runoff modelling; HEC-HMS; hydrological modelling; semi-arid watershed.

1. Introduction

Sustainable water resources management is currently facing increasing challenges driven by rapid urbanization, population growth, and the impacts of climate change. Changes in precipitation patterns, rising temperatures, and increasing climate variability can significantly affect the availability and variability of water resources (Barnett et al., 2005). In this context, hydrological models have become indispensable tools for understanding rainfall–runoff processes, supporting integrated watershed management, and improving the assessment and prediction of hydrological hazards such as floods (Beven, 2012; Gupta et al., 1999).

The accuracy of hydrological modelling largely depends on the quality and availability of precipitation data, which constitute the primary input for rainfall–runoff models. However, adequately characterizing the spatial and temporal variability of precipitation remains challenging when rain-gauge observations are limited or unevenly distributed (Maidment, 1993). To overcome these limitations, satellite precipitation products have become an increasingly important source of rainfall information, offering continuous observations with broad spatial coverage (Tang et al., 2013). Their use in hydrological modelling has expanded considerably over recent years, particularly for flood simulation and water resources assessment in data-scarce regions (Nguyen et al., 2018). Nevertheless, uncertainties associated with satellite precipitation estimates remain a major challenge and require careful evaluation before their application in operational hydrological studies (Beck et al., 2017; Nguyen et al., 2018). Although satellite precipitation products have been widely investigated in hydrological applications, relatively few studies have focused on the use of bias-corrected Precipitation Estimation from Remotely Sensed Information using Artificial Neural Networks–Cloud Classification System (PERSIANN-CCS) precipitation for event-based rainfall–runoff modelling in semi-arid Moroccan watersheds. Furthermore, the transferability of satellite precipitation products remains highly dependent on regional climatic and physiographic conditions, making local evaluations essential before their operational application for flood modelling and water resources management (Gebregiorgis & Hossain, 2015).

Against this background, the present study focuses on the Oued Nfifikh watershed, one of the watersheds within the Bouregreg–Chaouia Hydraulic Basin in northwestern Morocco, an area characterized by pronounced climatic variability and increasing pressure on water resources. The objective of this study is to evaluate the performance of observed rainfall and corrected PERSIANN-CCS satellite precipitation for event-based rainfall–runoff simulation using the HEC-HMS hydrological model. Simulated streamflows are compared with observed hourly discharge records to assess the capability of each rainfall dataset to reproduce the hydrological response of the watershed.

To enhance the reliability of the simulations, a modelling framework combining manual calibration, automatic calibration, model validation, and sensitivity analysis was implemented. The same calibration strategy and initial parameter values were adopted for both rainfall datasets to ensure a consistent and objective comparison of their hydrological performance. The outcomes of this study provide additional insight into the applicability of PERSIANN-CCS precipitation for event-based hydrological modelling in semi-arid Moroccan watersheds and may support future applications related to flood simulation and water resources management in regions where ground-based rainfall observations are limited.

2. Materials and Methods

2.1. Description of the Study Area

The study was conducted in the Oued Nfifikh watershed, located in northwestern Morocco (Figure 1). The watershed considered in this study is controlled by the Feddan Taba hydrometric station, which was adopted as the outlet for watershed delineation, resulting in a drainage area of approximately 644.42 km². Hydrologically, the watershed belongs to the Atlantic coastal watersheds, while administratively it forms part of the Bouregreg and Chaouia Hydraulic Basin, which is managed by the Bouregreg and Chaouia Hydraulic Basin Agency (ABHBC) (ABHBC, 2012). The basin is characterized by a semi-arid Mediterranean climate, with most precipitation occurring between autumn and spring and a dry summer season, while the average annual rainfall is approximately 400 mm (ABHBC, 2012; Merbouh et al., 2022). The topography is characterized by a progressive increase in elevation from the downstream coastal plain toward the southeastern upstream areas, reflecting the geomorphological features of the Atlantic coastal basins of northwestern Morocco (ABHBC, 2012). Geologically, the watershed belongs to the northwestern Moroccan Meseta and is mainly composed of Paleozoic basement rocks overlain by Triassic, Liassic and Quaternary sedimentary formations, including limestone, marl and sandstone

(Farki et al., 2012). Land use is dominated by agricultural areas, together with natural vegetation and localized urban settlements, which represent the main landscape units within the watershed (ABHBC, 2012; Merbouh et al., 2022).

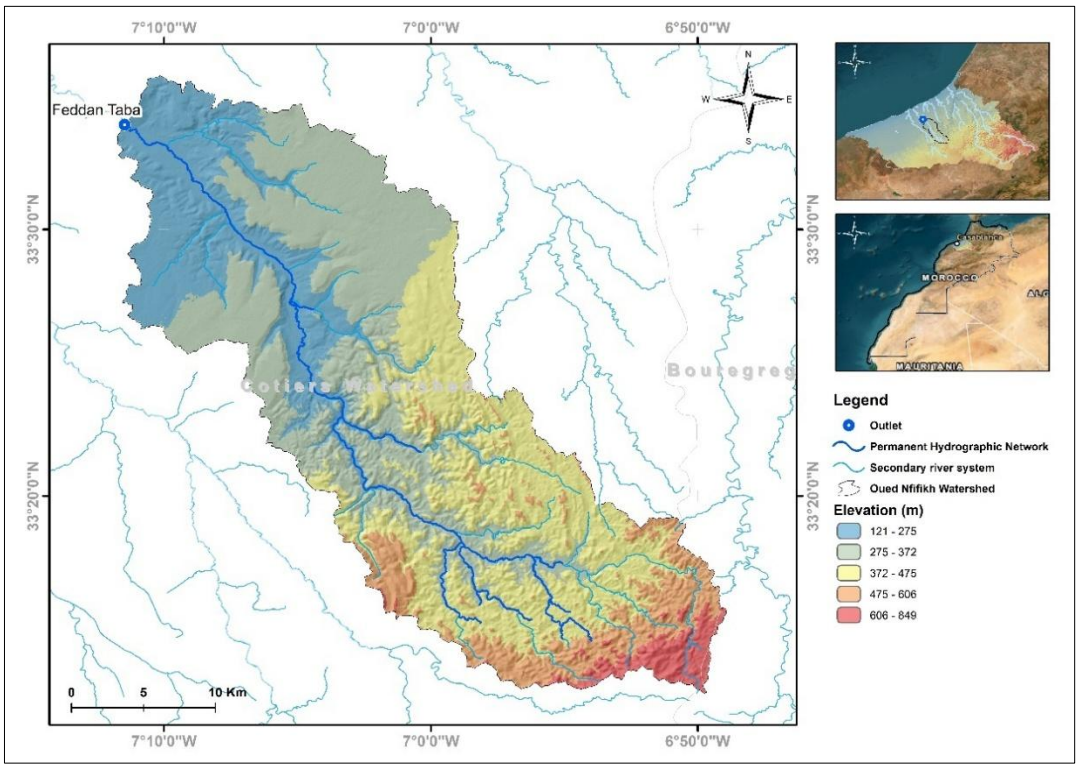


Fig. 1 *Geographical location of Oued Nfifikh watershed*

2.2. Datasets

Rainfall–runoff modeling using HEC-HMS requires several types of input data, including precipitation, streamflow, soil characteristics, land use/land cover (LULC), and topographic information. In this study, the datasets used mainly include observed and satellite-based precipitation data, as well as observed hourly streamflow data recorded at the Feddan Taba hydrometric station, which controls the Oued Nfifikh watershed. These datasets constitute the basis for the calibration and validation of the hydrological model. For each of the nine selected flood events, hourly observed rainfall, hourly PERSIANN-CCS rainfall, and hourly observed streamflow time series were extracted and used as input for the event-based HEC-HMS simulations.

2.2.1. Observed Rainfall Data

In this study, rainfall data were collected from four rain gauge stations located within and around the Oued Nfifikh basin, namely Feddan Taba, Melilla 1, Oulad Mhamed, and Ain Loudah (Figure 2 and Table 1). The selection of these stations was based on their influence on the precipitation regime, which governs the hydrological response of the basin. Feddan Taba also represents the outlet station where observed streamflow data were available. To account for the spatial variability of precipitation, the Thiessen polygon method was applied to calculate the basin-average weighted precipitation.

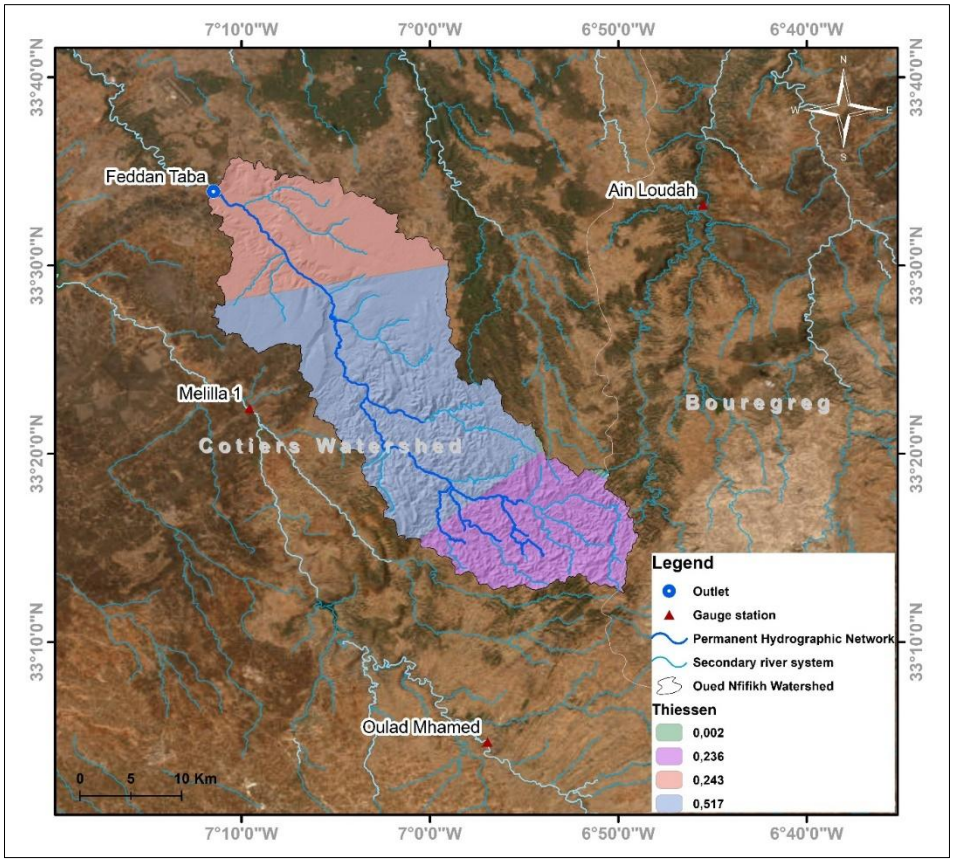


Fig. 2 *Spatial distribution of rain gauge stations and Thiessen polygons in the Oued Nfifikh watershed*

Table 1 *Stations used in this study*

Station Name	Longitudes	Latitudes
Ain Loudah	-6.758263	33.553582
Feddan Taba	-7.191283	33.565421
Ouled Mhammed	-6.948904	33.078265
Melilla	-7.159425	33.373546

2.2.2. Identification and Selection of Rainfall Events

The precipitation time series were analyzed to group consecutive rainy days into continuous rainfall events. A cumulative rainfall threshold of 30 mm was defined to retain only significant events considered capable of generating substantial runoff over the entire watershed. Initially, thirteen rainfall events satisfying this criterion were identified. However, four events were excluded due to incomplete rainfall records across the selected rain gauge stations. Based on this criterion, nine representative rainfall events covering the 2010–2016 period were selected. These events exhibit varying rainfall intensities and durations, reflecting the diversity of precipitation regimes within the basin (Table 2). For each selected event, the corresponding hourly rainfall and discharge time series were extracted and used as inputs for the event-based HEC-HMS simulations.

Table 2 *Selected rainfall events, duration, and cumulative rainfall*

Event No.	Start Date	End Date	Duration	Cumulative Rainfall (mm)
1	04/11/2014 06:00	06/11/2014 07:00	2 d 1 h	47.57
2	21/11/2014 07:00	07/12/2014 07:00	16 d	110.46
3	13/12/2014 07:00	17/12/2014 17:00	4 d 10 h	45.81
4	13/01/2015 07:00	24/01/2015 18:00	11 d 11 h	73.01
5	26/02/2016 07:00	29/02/2016 23:00	3 d 16 h	32.30
6	20/03/2016 08:00	24/03/2016 07:00	3 d 23 h	30.07
7	03/01/2010 07:00	15/01/2010 07:00	12 d 0 h	75.44

8	26/11/2010 08:00	08/12/2010 00:00	11 d 16 h	138.75
9	02/11/2011 07:00	08/11/2011 00:00	5 d 17 h	61.09

2.2.3. Satellite-Based Precipitation Data

In addition to in situ measurements, precipitation data from the PERSIANN-CCS (Precipitation Estimation from Remotely Sensed Information using Artificial Neural Networks–Cloud Classification System) satellite product were used. Developed by the Center for Hydrometeorology and Remote Sensing (CHRS) at the University of California, Irvine, PERSIANN-CCS provides near-real-time precipitation estimates with an hourly temporal resolution and a spatial resolution of 0.04°, making it suitable for hydrological applications in regions where ground-based observations are sparse or incomplete (Hong et al., 2004; Nguyen et al., 2019). A detailed description of the PERSIANN-CCS dataset, the preprocessing steps, the bias-correction methodology, and its validation against ground-based observations is provided by El Martili et al. (2025). In the present study, the corrected hourly PERSIANN-CCS precipitation data corresponding to the selected flood events were directly used as input to the HEC-HMS model, and the resulting streamflow simulations were compared with those obtained using observed rainfall.

2.2.4. Missing Data Processing

A specific procedure was applied to address the gaps identified in the observed rainfall time series, particularly at the Melilla station. The adopted method is based on a semi-empirical approach combining (i) the available daily rainfall totals at the target station and (ii) the instantaneous hourly time-step records from neighboring stations. Each missing value was estimated using a weighting factor derived from the ratio between the daily rainfall totals of the target station and those of the neighboring stations, and then adjusted using the available hourly observations. This approach allowed the preservation of the consistency of daily rainfall totals while reproducing the intra-daily variability required for rainfall–runoff modeling.

2.2.5. Observed Discharge Data

The observed hourly streamflow data were obtained from the Feddan Taba hydrometric station, located at the outlet of the basin (Figure 1). These time series, provided by the Bouregreg–Chaouia Hydraulic Basin Agency (ABHBC), occasionally exhibited irregular time steps (hourly, 4-hourly, or 6-hourly intervals). To ensure compatibility with hydrological simulations, the records were resampled to an hourly time step using linear interpolation. Each value was plotted and identified as either original or interpolated to ensure data traceability and to avoid any distortion of the simulated hydrographs.

2.3. HEC-HMS model construction

The Hydrologic Engineering Center–Hydrologic Modeling System (HEC-HMS) is a widely used modeling tool for simulating rainfall–runoff processes in watershed systems. It has been extensively applied in hydrological studies under various climatic and physiographic conditions, demonstrating satisfactory performance for both flood forecasting and water resources management (Halwatura & Najim, 2013; Hydrologic Engineering Center, 2023; Yusop et al., 2007).

In this study, HEC-HMS was developed to simulate rainfall–runoff processes in the Oued Nfifikh watershed. The model configuration included several components, namely the loss method, transform method, and baseflow method, which are required to represent the hydrological cycle from precipitation input to streamflow response at the basin outlet. The model was driven by both ground-based precipitation data, processed using the Thiessen polygon method, and bias-corrected satellite precipitation data derived from the PERSIANN-CCS product. Observed streamflow data from the Feddan Taba hydrometric station were used for model calibration and validation. This configuration enabled the assessment of the performance of observed and satellite-based precipitation datasets in reproducing flood hydrographs within the basin. The overall workflow of the HEC-HMS modelling framework adopted in this study is illustrated in Figure 3.

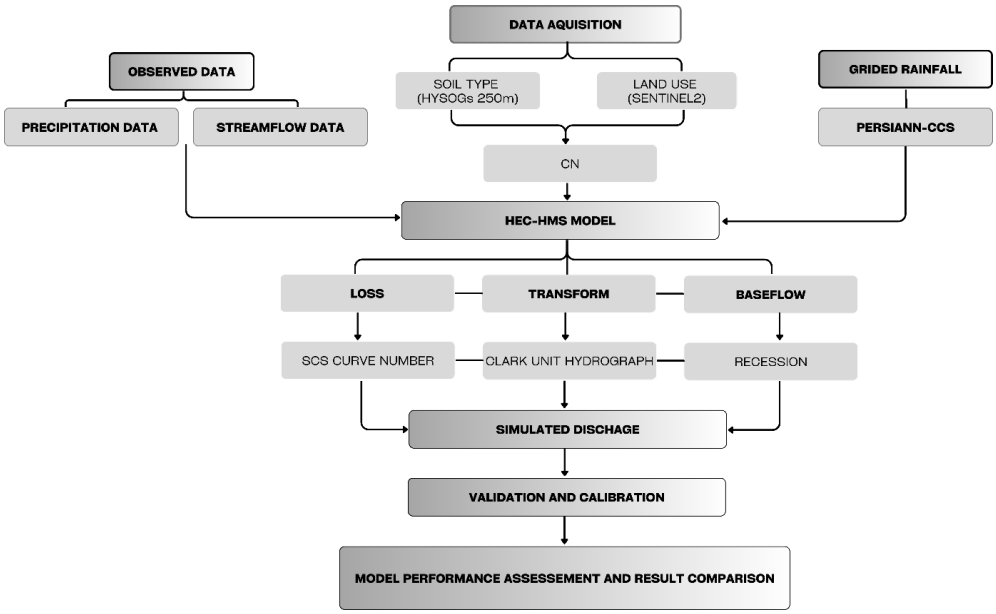
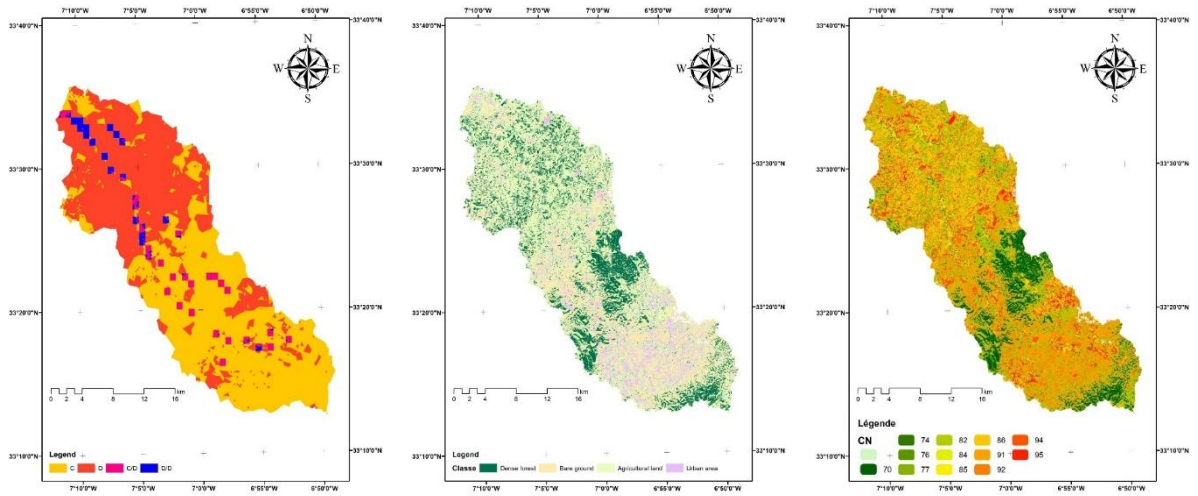


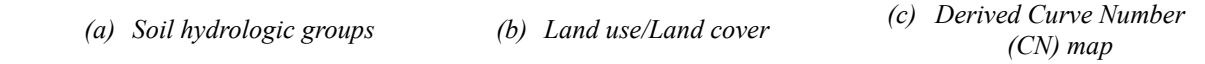
Fig. 3 *Workflow of the HEC-HMS rainfall–runoff modelling framework adopted in this study*

2.3.1. Loss Model

The Soil Conservation Service Curve Number (SCS-CN) method was adopted in HEC-HMS to estimate direct runoff from rainfall events. This approach establishes an empirical relationship between rainfall depth, land use/land cover (LULC), and hydrological soil groups, making it one of the most widely applied loss models in hydrological simulations (Mishra & Singh, 2003; USDA Soil Conservation Service [USDA-SCS], 1972). Curve Number (CN) values increase with runoff potential and decrease with infiltration capacity, providing a simple yet robust tool for representing watershed heterogeneity (Ponce & Hawkins, 1996).

In this study, the CN map was generated by integrating land use/land cover and soil type data within a GIS environment (Figure 4 (c)). Land use/land cover information was derived from a Sentinel-2 image acquired on April 17, 2015, processed through supervised classification and mosaicking techniques (Figure 4 (b)), whereas soil (Figure 4 (a)) data were obtained from the Global Hydrologic Soil Groups (HYSOGs250m) database (Ross et al., 2018). CN values for each soil–land use combination were assigned according to the tables provided in the USDA Soil Conservation Service Technical Release 55 (U.S. Department of Agriculture, Soil Conservation Service [USDA-SCS], 1986). The weighted Curve Number (CN) for the controls the Oued Nfifikh watershed was calculated as 84.40, indicating a moderately high runoff potential under average antecedent moisture conditions (AMC II). Furthermore, the proportion of impervious surfaces, mainly associated with urban areas, was estimated at 10.92%, highlighting the influence of urbanization on runoff generation and the reduction of infiltration capacity within the basin.





(a) Soil hydrologic groups *(b) Land use/Land cover* *(c) Derived Curve Number (CN) map*

Fig. 4 *Generation of the Curve Number (CN) map*

The initial abstraction parameter (Ia) is a key component of the SCS Curve Number (SCS-CN) model, as it represents the initial hydrological losses (interception, surface depression storage, and infiltration) occurring before the onset of direct runoff. In the classical formulation, Ia is expressed as a fraction of the potential maximum retention capacity of the watershed (S), according to the following relationship:

$$Ia = \lambda \times S,\ S = \frac{25400}{CN} - 254$$

Where CN represents the Curve Number and λ is a proportionality factor. The Soil Conservation Service (USDA-SCS, 1972) recommends a default value of λ = 0.20, leading to the relationship Ia = 0.2 × S. However, several studies have reported that this standard value may overestimate initial abstraction, leading to an underestimation of direct runoff. Hawkins et al. (2009) and Mishra and Singh (2003) showed that λ depends on watershed characteristics and may vary substantially among watersheds. Hawkins et al. (2009) reported that λ = 0.05 provided a better fit for many watersheds than the conventional value of 0.20. Elhakeem and Papanicolaou (2009) and Mishra et al. (2008) also demonstrated that lower λ values can improve runoff simulations in some watersheds.

In the present study, the basin-wide Curve Number was estimated at 84.40, corresponding to a potential maximum retention capacity of:

$$S = \frac{25400}{84{,}40} - 254$$

Consequently, adopting the conventional assumption (λ = 0.20) yielded an initial abstraction value of:

$$Ia = 0.2 \times 46{,}95 \approx 9.39 \text{ mm}$$

This value was used as the initial estimate for model calibration, while the final parameter values were subsequently optimized during the calibration process.

2.3.2. Transform Model

The transformation of excess rainfall into direct runoff was simulated using the Clark Unit Hydrograph (Clark UH) method implemented in HEC-HMS. The Clark Unit Hydrograph conceptualizes the rainfall–runoff transformation by combining runoff translation through a time–area relationship with linear storage routing, thereby accounting for both the travel time of runoff within the watershed and the attenuation of the flood wave before it reaches the basin outlet. Owing to its simplicity and its ability to reproduce flood hydrographs satisfactorily, the Clark Unit Hydrograph has been widely applied in event-based hydrological modelling (Clark, 1945; Hydrologic Engineering Center, 2023).

The Clark Unit Hydrograph requires two principal parameters: the Time of Concentration (Tc) and the Storage Coefficient (Rs). The Time of Concentration (Tc) represents the travel time required for runoff generated at the hydraulically most distant location of the watershed to reach the outlet. It is one of the principal parameters controlling the timing of the simulated flood hydrograph. The Storage Coefficient represents the temporary storage of water within the watershed and drainage network, influencing the attenuation and recession of the simulated hydrograph (Chow et al., 1988). In many hydrological applications, the Time of Concentration is estimated using empirical equations based on watershed morphometric characteristics. However, the applicability of these equations strongly depends on the physical characteristics of the watershed and may lead to considerable differences in the estimated values. Therefore, in the present study, an initial Time of Concentration (Tc) of 19 h was adopted as the starting value for the calibration procedure. The time of concentration was empirically and analytically validated by evaluating the temporal offset between the rainfall hyetograph and the corresponding runoff hydrograph, ensuring the calculated travel time reflects the actual catchment response during the monitored storm events. The Storage Coefficient (Rs) was also assigned an initial value and subsequently refined during calibration.

Finally, both Tc and Rs were adjusted through manual and automatic event-based calibration to achieve the best agreement between the simulated and observed hydrographs in terms of peak timing and hydrograph shape. This calibration strategy allowed the transformation model to accurately represent the rainfall–runoff response of the controls the Oued Nfifikh watershed (Hydrologic Engineering Center, 2023).

2.3.3. Baseflow model

Baseflow was simulated using the Recession model implemented in HEC-HMS. This conceptual approach represents the contribution of groundwater to streamflow by assuming that baseflow decreases exponentially after a rainfall event. Owing to its simplicity and its ability to satisfactorily reproduce the recession limb of streamflow hydrographs, the Recession model has been widely applied in event-based hydrological modelling (Chow et al., 1988; Hydrologic Engineering Center, 2023).

The Recession model is defined by three principal parameters: the initial discharge (Q_0), the recession constant (Rc), and the ratio to peak (Td). The initial discharge represents the contribution of baseflow at the beginning of the simulation. The recession constant is a dimensionless parameter ranging between 0 and 1 that controls the rate of baseflow decline during the recession phase. The ratio to peak parameter, also ranging between 0 and 1, defines the threshold, expressed as a fraction of the simulated peak discharge, at which the recession model resumes its contribution after the passage of the flood peak (Hydrologic Engineering Center, 2023).

The Recession model parameters were initially assigned using starting values consistent with commonly adopted practices in HEC-HMS applications. These values were subsequently adjusted during manual and automatic calibration procedures to achieve the best agreement between simulated and observed hydrographs. This calibration strategy improved the representation of baseflow contribution and the recession phase of the simulated hydrographs**.**

2.4. Model calibration and validation

Model calibration and validation are essential steps in hydrological modelling, as they assess the ability of a model to reliably reproduce the hydrological response of a watershed. Calibration consists of adjusting the model parameters to minimize the discrepancies between simulated and observed streamflow, whereas validation evaluates the predictive capability of the calibrated model using independent events that were not involved in the calibration process (Refsgaard, 1997).

In this study, an event-based calibration approach was adopted using the HEC-HMS model. The hydrological parameters were first addusted through manual calibration and subsequently refined using the automatic optimization module to achieve the best agreement between simulated and observed hydrographs. This procedure was initially performed using the observed rainfall data. The PERSIANN-CCS precipitation data were then calibrated following the same methodology and using the same initial parameter values, thereby ensuring a consistent comparison between the two rainfall data sources.

A total of nine flood events were selected based on the quality and availability of the hydrometeorological data. Among them, six events (66.7%) were used for model calibration, whereas the remaining three events (33.3%) were reserved for model validation. The calibration events, covering the 2014–2016 period, were selected to represent different rainfall intensities and hydrological responses of the watershed. The validation events, covering the 2010–2011 period, were independent from those used during calibration and served to evaluate the predictive capability of the calibrated model under different hydrological conditions. Therefore, the selection of events was primarily based on their hydrological representativeness and on data quality and availability rather than on chronological order.

Following the calibration phase, the optimized parameter values obtained for the six calibration events were averaged to derive a single representative parameter set for the watershed. This parameter set was subsequently applied during the validation phase for the three independent events using both observed rainfall and PERSIANN-CCS precipitation.

2.5. Model performance evaluation

2.5.1. Statistical Metrics

The evaluation of hydrological model performance is a fundamental step in determining the reliability of rainfall–runoff simulations and the model's ability to reproduce the hydrological response of a watershed. In this study, the performance of the HEC-HMS model was assessed by comparing simulated and observed streamflow hydrographs at the Feddan Taba gauging station. The evaluation was carried out for simulations driven by both observed rainfall and PERSIANN-CCS precipitation, allowing the influence of the rainfall data source on model performance to be assessed. To provide a comprehensive evaluation, six complementary statistical indicators were employed: the Nash–Sutcliffe Efficiency (NSE), Root Mean Square Error (RMSE), Mean Absolute Error (MAE), Percentage Bias (PBIAS), the Pearson Correlation Coefficient (R), and the Coefficient of Determination (R^2). These indicators

are widely recognized in hydrological modelling because they evaluate different aspects of model performance, including prediction accuracy, error magnitude, systematic bias, and the agreement between simulated and observed streamflow (Gupta et al., 2009; Legates & McCabe, 1999; Moriasi et al., 2007). The mathematical expressions of the statistical indicators used in this study are presented in Table 3.

Table 3 *Statistical indicators used for model performance evaluation*

Indicators	Equation	Possible values	Optimal value	References
The correlation coefficient (R)	$\frac{\sum_{i=1}^{n}(Qobs - Qobs)\sum_{i=1}^{n}(Qsim - Qsim)}{\sqrt{\sum_{i=1}^{n}(Qobs - Qobs)^2}\sqrt{\sum_{i=1}^{n}(sim - Qsim)^2}}$	-1 to 1	1	Legates and McCabe (1999)
Coefficient of Determination (R^2)	$R^2 = R^2$ (or calculated directly from regression	-1 to 1	1	Legates and McCabe (1999)
Root mean square error (RMSE)	$\sqrt{\frac{\sum_{i=1}^{n}(Qsim - Qobs)^2}{n}}$	0 to +∞	0	Chai and Draxler (2014)
Nash Sutcliffe model Efficiency coefficient (NSE)	$1 - \frac{\sum_{i=1}^{n}(Qobs - Qsim)^2}{\sum_{i=1}^{n}(Qobs - Qobs)^2}$	−∞ to 1	1	Nash and Sutcliffe (1970); Moriasi et al. (2007)
Percentage RBiais	$\frac{\sum_{i=1}^{n} Qobs - Qsim}{\sum_{i=1}^{n} Qobs} * 100$	0 to +∞	0	Gupta et al. (1999); Moriasi et al. (2007)
Mean Absolute Error (MAE)	$\frac{1}{N}\sum_{i=1}^{n} \lvert Qsim, i - Qobs, i \rvert$	0 to +∞	0	Willmott and Matsuura (2005)

3. Results and Discussion

3.1. Sensitivity Analysis

To evaluate the influence of the hydrological parameters on the performance of the HEC-HMS model, a One-At-a-Time (OAT) sensitivity analysis was conducted by varying one parameter while keeping all other parameters fixed at their calibrated values. The Curve Number (CN) was varied within a range of ±10%, whereas the remaining parameters, namely Initial Abstraction (Ia), Time of Concentration (Tc), Storage Coefficient, Initial Discharge, Recession Constant, and Ratio to Peak, were varied within ±30%, representing physically realistic ranges.

Figure 5 illustrates the variation of the Nash–Sutcliffe Efficiency (NSE) in response to changes in the model parameters. The results clearly indicate that the Curve Number is the most sensitive parameter. Although its variation was limited to ±10%, small changes in CN produced substantial variations in model performance, highlighting its dominant role in controlling runoff generation. The Initial Abstraction was identified as the second most influential parameter, while the Time of Concentration and Storage Coefficient exhibited moderate sensitivity. In contrast, the baseflow-related parameters (Initial Discharge, Recession Constant, and Ratio to Peak) had only a limited influence on the overall model performance. The small changes in NSE observed for these parameters around the reference value indicate that the model is relatively insensitive to variations in the flow routing and recession processes.

The sensitivity analysis confirms that particular attention should be paid to the Curve Number and Initial Abstraction during model calibration, as these parameters have the greatest influence on the simulated hydrological response, while the remaining parameters mainly affect the timing of the hydrograph.

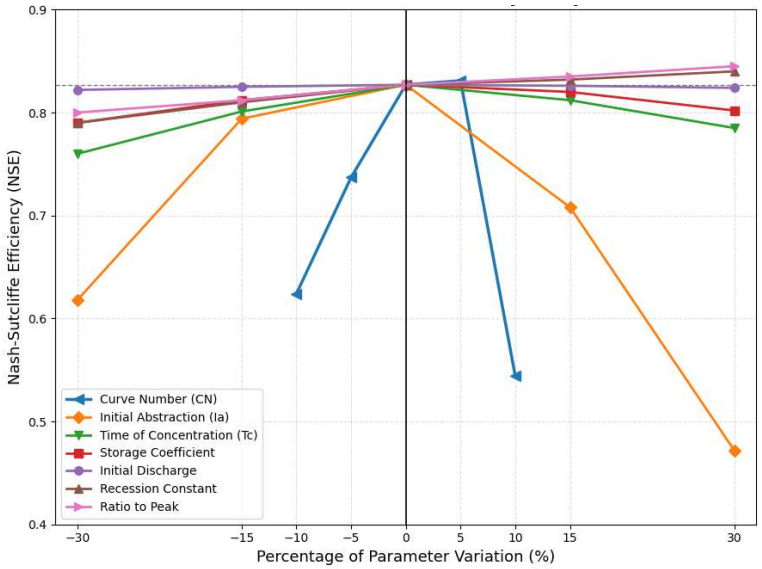


Fig. 5 *Sensitivity analysis of the calibrated hydrological parameters based on the Nash–Sutcliffe Efficiency (NSE)*

3.2. Manual calibration and validation using observed rainfall

The performance of the HEC-HMS model following the manual calibration procedure using observed rainfall data is summarized in Table 4. Overall, the model reproduced the rainfall–runoff response of the Oued Nfifikh watershed with satisfactory accuracy for both the calibration and validation events. Nevertheless, the simulation performance varied from one event to another, reflecting differences in rainfall characteristics and antecedent hydrological conditions.

During the calibration phase (E1–E6), the Nash–Sutcliffe Efficiency (NSE) ranged from 0.327 to 0.828. The highest performance was obtained for Event E3 (NSE = 0.828), which also exhibited a low RMSE (0.4) and a small bias (PBIAS = −5.98%), indicating a good overall fit according to these performance indicators, although the flood peak was underestimated. Conversely, Event E5 showed the lowest performance (NSE = 0.327), suggesting that this event was more difficult to reproduce because of its specific hydrometeorological characteristics.

The comparison between observed and simulated peak discharges indicates that the model generally reproduced the magnitude of the flood peaks, although some discrepancies remained. For example, the simulated peak discharge reached 28.1 m³/s compared with an observed value of 40.0 m³/s for Event E3, whereas Event E8 showed an overestimation of the flood peak (137.4 m³/s versus 114.0 m³/s). Similar trends were observed for runoff volumes. The simulated runoff volume for Event E3 (7.23 Mm³) was close to the observed value (6.78 Mm³), while larger differences were obtained for Event E8, where the simulated volume reached 21.19 Mm³ compared with an observed volume of 15.08 Mm³. These differences are consistent with the statistical performance indices reported in Table 4.

The validation results (E7–E9) showed variable performance of the calibrated parameter set across independent rainfall events. In particular, Event E7 achieved an NSE of 0.796 with a relatively low bias (8.38%), indicating that the calibrated parameters reproduced this independent event with satisfactory overall performance. Although lower performances were obtained for Event E9, the overall agreement between simulated and observed hydrographs remained acceptable.

The manually calibrated parameter set therefore provided a reasonable representation of the watershed response and was subsequently adopted as the initial parameter set for the automatic calibration procedure and for the evaluation PERSIANN-CCS rainfall product.

Table 4 *Performance of the manually calibrated model using observed rainfall for the calibration and validation events*

Event	Phase	NSE	RMSE	PBIAS (%)	Peak discharge (Obs.) (m^3/s)	Peak discharge (Sim.) (m^3/s)	Runoff volume (Obs.) (Mm^3)	Runoff volume (Sim.) (Mm^3)
E1	Calibration	0.609	0.6	24.61	42.0	22.8	1.59	2.23
E2	Calibration	0.679	0.6	16.15	75.0	39.0	11.20	14.33
E3	Calibration	0.828	0.4	-5.98	40.0	28.1	6.78	7.23
E4	Calibration	0.577	0.7	8.43	28.0	23.7	6.90	8.45
E5	Calibration	0.327	0.8	39.60	24.6	20.7	2.43	3.60
E6	Calibration	0.524	0.7	49.59	31.5	16.7	2.41	3.63
E7	Validation	0.796	0.5	8.38	86.0	66.8	22.27	24.31
E8	Validation	0.713	0.5	37.44	114.0	137.4	15.08	21.19
E9	Validation	0.333	0.8	12.82	30.0	23.0	3.52	5.01

3.3. Automatic calibration and validation using observed rainfall

The automatic calibration procedure was subsequently performed to refine the parameter values obtained during the manual calibration stage. The objective was to improve the agreement between simulated and observed hydrographs while maintaining physically meaningful parameter values. The optimized parameter set was then tested using the six calibration events and three independent validation events.

Table 5 summarizes the statistical performance of the automatically calibrated model, while Figure 6 compares the observed and simulated hydrographs for both the calibration (E1–E6) and validation (E7–E9) periods. The effect of automatic calibration varied across events, with improvements in NSE for some events and lower values for others compared with manual calibration. During calibration, the highest performance was achieved for Event E3 (NSE = 0.881), whereas Event E5 showed the lowest performance (NSE = 0.268), reflecting the greater difficulty in reproducing this particular flood event. During validation, Event E8 achieved the highest NSE (0.862), whereas Event E9 showed substantially lower performance (NSE = 0.312), indicating variable performance across independent events.

The complementary performance indicators provide further insight into model performance. The correlation coefficients (R) and coefficients of determination (R^2) indicate a strong association between observed and simulated streamflow for several events. Meanwhile, RMSE and MAE quantify simulation errors, and PBIAS provides information on the magnitude and direction of the overall bias.

The hydrographs presented in Figure 6 support these statistical results. In most cases, the model reproduced the temporal evolution of streamflow, including the timing of the flood peak, the recession limb, and the overall hydrograph shape. The closest agreement between observed and simulated hydrographs was obtained for Events E2, E3, E7, and E8, whereas larger differences were observed for Events E5, E6, and E9, reflecting the greater difficulty in reproducing the hydrological response of these events.

A comparison of peak discharge and runoff volume provides additional insight into the model behaviour. For Event E3, the simulated peak discharge reached 32 m^3/s, compared with an observed value of 40 m^3/s, while the simulated runoff volume (8 Mm^3) remained close to the observed volume (6 Mm^3). Similarly, for Event E8, the simulated peak discharge (112 m^3/s) was very close to the observed value (114 m^3/s), with runoff volumes of 17 Mm^3 and 15 Mm^3, respectively. Although larger differences were observed for some events, particularly Event E7, where the simulated runoff volume reached 26 Mm^3 compared with 22 Mm^3 observed, the model generally reproduced both flood magnitude and runoff volume with satisfactory accuracy.

Taken together, the automatic calibration improved the representation of the watershed response, achieving satisfactory performance for most events, although some discrepancies between observed and simulated flows remained.

Table 5 Performance of the HEC-HMS model after automatic calibration and validation using observed rainfall

Event	Phase	NSE	RMSE	PBIAS (%)	MAE	R	R^2	Peak discharge (Obs.	Peak discharge (Sim.) (m^3/s)	Runoff volume (Obs.) (Mm^3)	Runoff volume (Sim.

								) (m^3/s)			) (Mm^3)
E1	Calibration	0.5899	6.959	42.80	4.733	0.857	0.734	42	30	1	2
E2	Calibration	0.7122	5.900	25.87	4.316	0.872	0.760	75	45	12	15
E3	Calibration	0.8808	3.682	5.94	2.377	0.944	0.891	40	32	6	8
E4	Calibration	0.5377	3.927	26.04	2.917	0.822	0.676	28	23	7	9
E5	Calibration	0.2676	6.638	46.39	4.654	0.788	0.621	24	21	2	3
E6	Calibration	0.5067	4.494	56.03	3.097	0.892	0.796	31	19	2	3
E7	Validation	0.7593	9.079	23.71	6.069	0.922	0.851	86	70	22	26
E8	Validation	0.8623	8.666	20.49	5.716	0.937	0.878	114	112	15	17
E9	Validation	0.3116	6.703	7.37	4.649	0.760	0.578	30	23	3	4

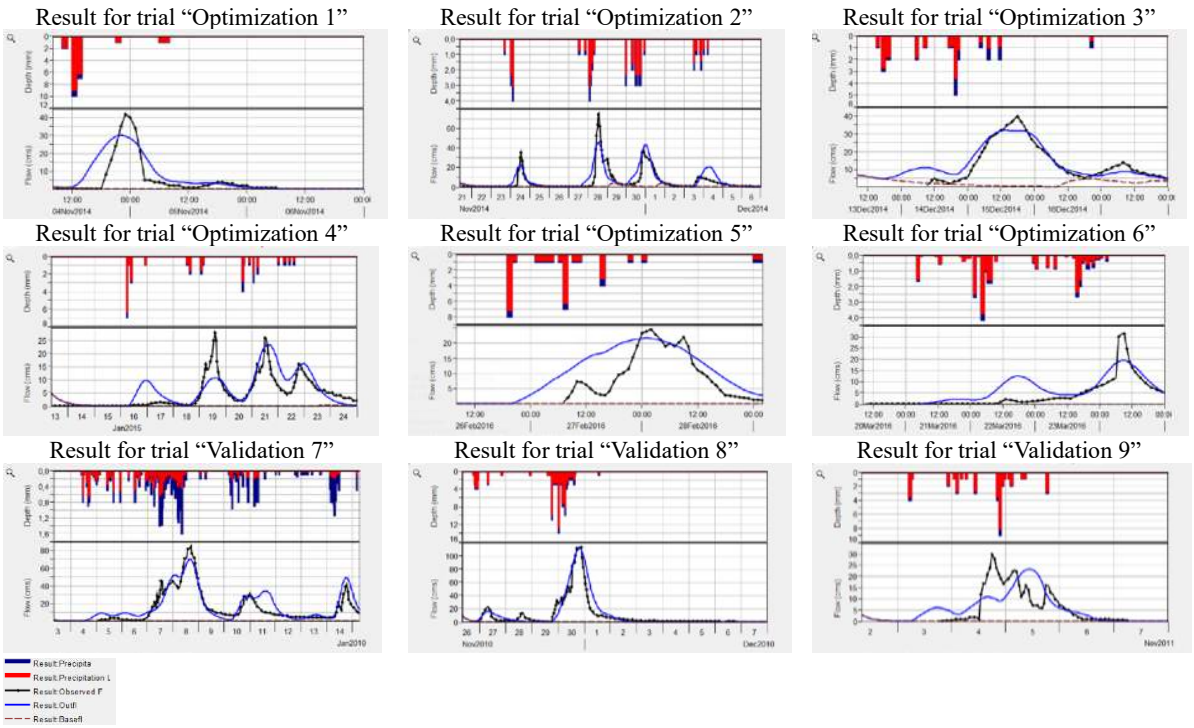


Fig. 6 *Observed and simulated hydrographs for calibration (E1–E6) and validation (E7–E9) events after automatic calibration*

3.4. Model simulation using PERSIANN-CCS rainfall

To further evaluate the applicability of satellite precipitation for rainfall–runoff modelling, the optimized parameter set obtained from the automatic calibration using observed rainfall was directly applied to simulations driven by PERSIANN-CCS rainfall. No additional parameter adjustment was performed, ensuring that any differences between the simulations resulted solely from the rainfall input rather than from recalibration of the hydrological model.

Table 6 summarizes the statistical performance obtained using PERSIANN-CCS rainfall, while Figure 7 compares the simulated and observed hydrographs for both the calibration (E1–E6) and validation (E7–E9) events.

As shown in Table 6, the simulations driven by PERSIANN-CCS rainfall generally reproduced the main characteristics of the observed streamflow, with performance varying across events. The hydrographs generally captured the timing of flood peaks, the recession limbs, and the overall flood dynamics, although the level of agreement varied among events, reflecting differences in the ability of the satellite product to represent individual rainfall events.

During the calibration period (E1–E6), the model showed satisfactory to excellent performance. The best result was obtained for Event E3 (NSE = 0.906), whereas the lowest performance was observed for Event E1 (NSE = 0.457). Based on the statistical indicators, Events E3, E4, and E6 exhibited the best overall performance during calibration, while Events E1 and E2 were reproduced with lower accuracy, suggesting greater uncertainty in the satellite-derived rainfall estimates for these storms.

A similar trend was observed during the validation period. The highest validation performance was achieved for Event E8 (NSE = 0.869), while Event E9 also produced acceptable results. Although some discrepancies remained during the recession period, the overall timing and shape of the simulated hydrographs were generally well reproduced.

The complementary statistical indicators further support the assessment of model performance. The correlation coefficients (R) and coefficients of determination (R^2) indicate a strong association between observed and simulated streamflow for several events. RMSE and MAE quantify the remaining simulation errors, while PBIAS provides additional insight into the magnitude and direction of the overall bias.

These statistical results are consistent with the hydrographs presented in Figure 7. The overall agreement between the simulated and observed hydrographs was particularly good for Events E3 and E8 in terms of flood timing and hydrograph shape, although the peak discharge remained underestimated for Event E8. Events E4 and E6 also reproduced the general flood dynamics satisfactorily despite some differences in peak magnitude. Larger discrepancies were observed for Events E1, E2, E5, and E7, while Event E9 showed an acceptable overall agreement despite a slight underestimation of the flood peak.

This behaviour is also reflected in the peak discharge and runoff volume estimates. For Event E3, the simulated peak discharge reached 34 m^3/s, compared with 40 m^3/s observed, while the simulated runoff volume (7 Mm^3) remained close to the observed value (6 Mm^3). During validation, Event E8 produced runoff volumes of 14 Mm^3 and 15 Mm^3 for the simulated and observed hydrographs, respectively, although the peak discharge was underestimated (78 m^3/s versus 114 m^3/s). Larger differences were observed for Event E7, where both the simulated peak discharge (50 m^3/s) and runoff volume (18 Mm^3) were lower than the corresponding observed values (86 m^3/s and 22 Mm^3).

Overall, these results demonstrate the potential of the PERSIANN-CCS product to drive HEC-HMS simulations without recalibration, with satisfactory performance for several events. This approach offers a promising alternative for event-based hydrological modelling, particularly in watersheds where rain gauge observations are limited.

Table 6 *Automatic calibration and validation results using PERSIANN-CCS rainfall*

Event	Phase	NSE	RMSE	PBIAS (%)	MAE	R	R^2	Peak discharge (Obs.) (m^3/s)	Peak discharge (Sim.) (m^3/s)	Runoff volume (Obs.) (Mm^3)	Runoff volume (Sim.) (Mm^3)
E1	Calibration	0.4567	8.0099	53.37	5.5043	0.7760	0.6022	42	31	1	2
E2	Calibration	0.5272	7.5623	49.82	4.4034	0.7868	0.6191	75	41	12	17

E 3	Cali brat ion	0.9060	3.268 5	5.39	2.701 1	0.9544	0.911 0	40	34	6	7
E 4	Cali brat ion	0.6033	3.632 8	-9.95	2.502 5	0.7864	0.618 4	28	20	7	6
E 5	Cali brat ion	0.4886	5.546 7	13.55	4.597 7	0.7298	0.532 6	24	17	2	2
E 6	Cali brat ion	0.5082	4.474 0	16.33	2.439 8	0.7212	0.520 2	31	14	2	2
E 7	Vali dati on	0.7097	9.979 7	-18.56	6.546 2	0.8765	0.768 2	86	50	22	18
E 8	Vali dati on	0.8689	8.487 1	-12.29	5.231 6	0.9395	0.882 7	114	78	15	14
E 9	Vali dati on	0.6326	4.933 4	-1.73	3.276 5	0.7971	0.635 4	30	22	3	3

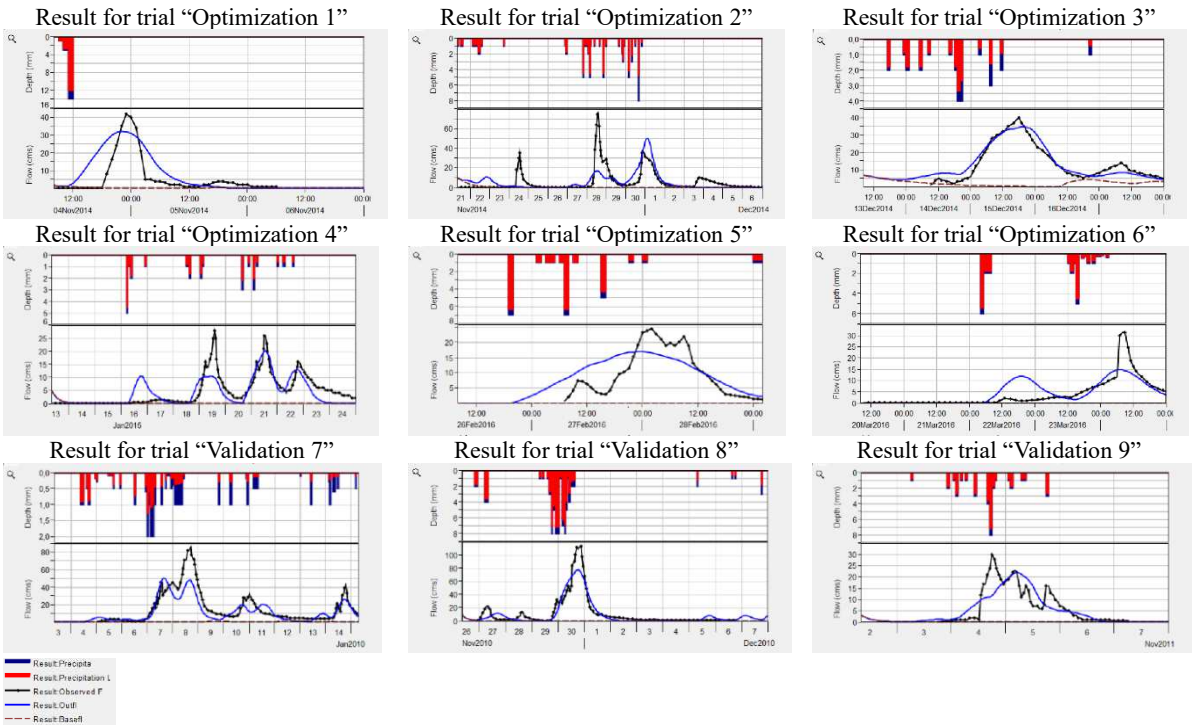


***Fig.** 7 Observed and simulated hydrographs using PERSIANN-CCS rainfall for calibration (E1–E6) and validation (E7–E9) events.*

3.5. Event-based comparison of model simulations using observed and PERSIANN-CCS rainfall

To directly assess the influence of the rainfall source on model performance, the statistical indicators obtained using observed rainfall and PERSIANN-CCS precipitation were compared for each flood event. Since the same calibrated parameter set was used for both simulations, the differences in model performance can be attributed exclusively to the rainfall input. The corresponding results are summarized in Table 7.

The comparison shows that the relative performance of the two rainfall datasets varies from one event to another. Simulations driven by observed rainfall produced better results for Events E1, E2, and E7, whereas PERSIANN-CCS performed better for Events E3, E4, E5, E8, and E9. For Event E6, both rainfall datasets yielded nearly identical performance.

These results indicate that neither rainfall dataset consistently outperformed the other across all flood events. Instead, model performance depended on the characteristics of each event and on the ability of each rainfall dataset to represent the corresponding precipitation pattern. The better performance of PERSIANN-CCS for five of the nine events highlights its potential as an alternative rainfall input for event-based hydrological modelling in the study watershed.

Table 7 *Event-based comparison between simulations using observed rainfall and PERSIANN-CCS precipitation*

Event	NSE OBS	NSE SAT	RMSE OBS	RMSE SAT	PBIAS OBS	PBIAS SAT	Better Performance
E1	0.5899	0.4567	6.959	8.010	42.80	53.37	Observed
E2	0.7122	0.5272	5.900	7.562	25.87	49.82	Observed
E3	0.8808	0.9060	3.682	3.269	5.94	5.39	Satellite
E4	0.5377	0.6033	3.927	3.633	26.04	-9.95	Satellite
E5	0.2676	0.4886	6.638	5.547	46.39	13.55	Satellite
E6	0.5067	0.5082	4.494	4.474	56.03	16.33	Equivalent
E7	0.7593	0.7097	9.079	9.980	23.71	-18.56	Observed
E8	0.8623	0.8689	8.666	8.487	20.49	-12.29	Satellite
E9	0.3116	0.6326	6.703	4.933	7.37	-1.73	Satellite

3.6. Overall statistical performance

To complement the event-based analysis, all simulated and observed streamflow values were combined to provide an overall assessment of model performance for both rainfall datasets. Figure 8 presents the scatter plots obtained for the calibration and validation periods using observed rainfall and PERSIANN-CCS precipitation, while the corresponding mean statistical indicators are summarized in Table 8.

Overall, the scatter plots show a clear positive relationship between observed and simulated streamflow for both rainfall datasets. Most data points are distributed around the 1:1 line, indicating that the HEC-HMS model is able to reproduce the general rainfall–runoff behaviour of the watershed under both calibration and validation conditions. A wider dispersion is observed for the highest flows, reflecting the greater uncertainty associated with peak discharge simulation.

The statistical indicators are consistent with these graphical observations. Using observed rainfall, the model achieved slightly better overall performance during calibration, whereas simulations driven by PERSIANN-CCS precipitation produced comparable results during validation. The two rainfall datasets yielded comparable mean NSE values, while differences in RMSE, PBIAS, and R^2 reflected variations in their overall simulation performance.

The mean statistical indicators presented in Table 8 further confirm these findings. Although differences are observed for individual flood events, the overall performance obtained with the PERSIANN-CCS product is comparable to that achieved using observed rainfall. These findings demonstrate the potential of the satellite precipitation product to reproduce the rainfall–runoff response of the Feddan Taba watershed and support its use as an alternative rainfall input for hydrological modelling.

Table 8 *Mean performance statistics for observed rainfall and PERSIANN-CCS precipitation*

Rainfall data	Simulation	Mean NSE	Mean RMSE	Mean PBIAS (%)	Mean R^2
Observed	Calibration (E1-E6)	0.582	5.27	33.18	0.695
Observed	Validation (E7-E9)	0.644	8.15	17.19	0.696
PERSIANN-CCS	Calibration (E1-E6)	0.582	5.42	21.42	0.634
PERSIANN-CCS	Validation (E7-E9)	0.737	7.80	−10.86	0.762

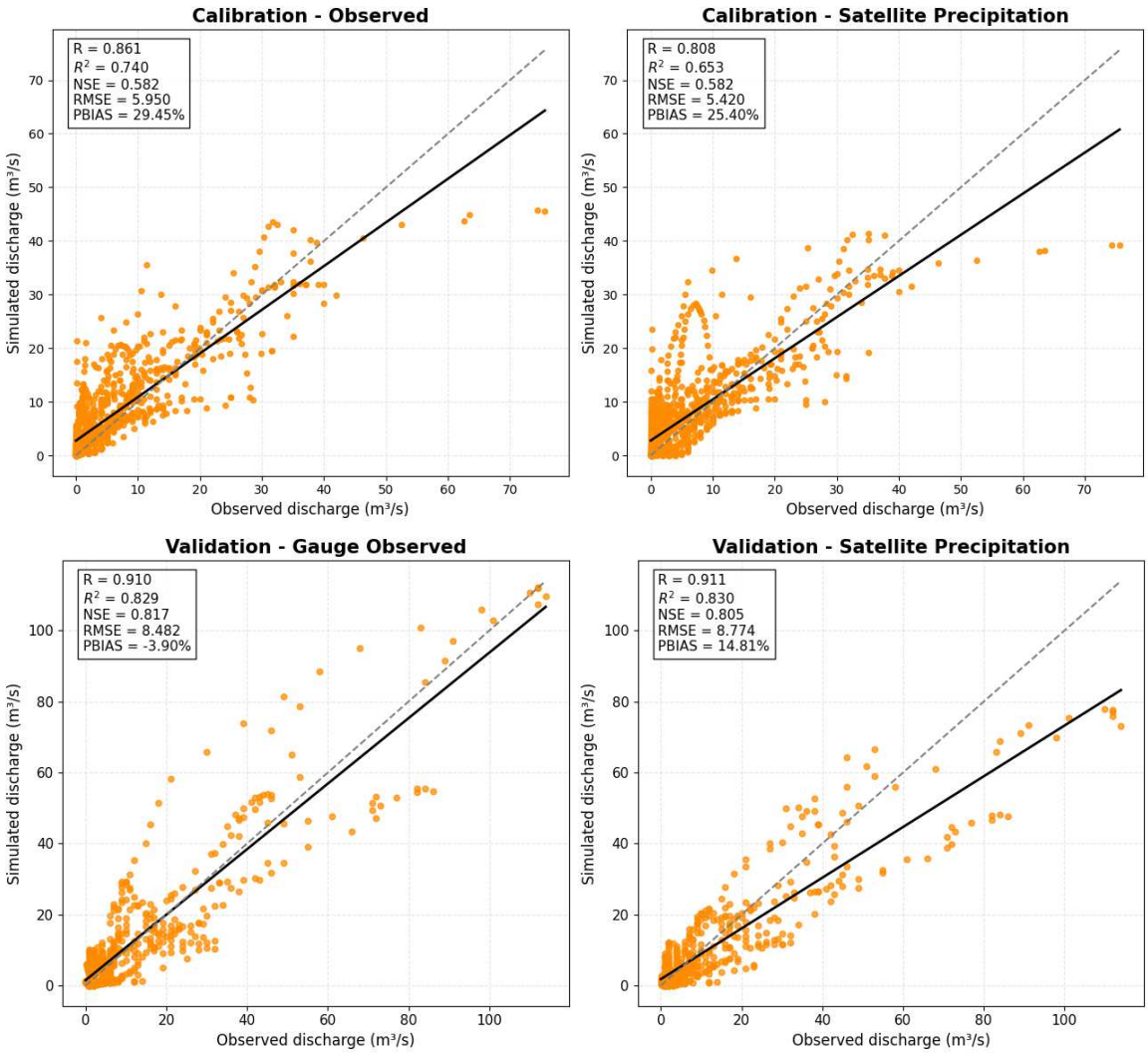


Fig. 8 *Scatter plots of observed versus simulated streamflow for calibration and validation using observed rainfall and PERSIANN-CCS precipitation*

3.7. Comparison with other studies

The results obtained in this study are consistent with previous research demonstrating that satellite precipitation products can provide reliable rainfall inputs for event-based hydrological modelling in regions where rain-gauge observations are sparse. However, their performance remains strongly influenced by watershed characteristics, climatic conditions, rainfall variability, and the quality of the satellite precipitation estimate.

In Morocco, several studies have investigated the potential of satellite-based precipitation products for hydrological applications. Tramblay et al. (2016) evaluated satellite-based rainfall products for hydrological modelling in Morocco and found that TRMM-3B42 v7 reproduced monthly flows more satisfactorily than daily flows in a northern Moroccan watershed. Saouabe et al. (2020) assessed the GPM-IMERG precipitation product for flood modelling in a semi-arid mountainous basin in Morocco. These studies highlight the potential of satellite precipitation products for hydrological modelling while emphasizing the importance of evaluating their performance at the temporal scales relevant to flood simulation.

Comparable conclusions have also been reported in other regions of the world. Bedada (2025) demonstrated that CHIRPS and PERSIANN-CDR provided satisfactory runoff simulations in Ethiopia after appropriate model calibration, while Dahal and Kojima (2025) and Llauca et al. (2024) reported reliable flood simulations using HEC-HMS in Bhutan and the Peruvian Andes, respectively. Likewise, Tedla et al. (2023) showed that satellite precipitation products can effectively support flood modelling in data-scarce regions, although their performance varies according to the rainfall event and the satellite product used. More generally, Gebregiorgis and Hossain

(2013) emphasized that the uncertainty associated with satellite precipitation is closely related to topography and climatic conditions, explaining why the performance of a given product differs from one watershed to another.

The present study extends these previous findings by directly evaluating the influence of the rainfall source while keeping the hydrological model unchanged. The same calibrated HEC-HMS parameter set was used for simulations driven by both observed rainfall and bias-corrected PERSIANN-CCS precipitation, ensuring that the observed differences were exclusively related to the rainfall input. The results obtained in this study support the applicability of PERSIANN-CCS precipitation for event-based hydrological modelling in semi-arid environments. They also demonstrate its potential as a reliable rainfall source for watersheds where ground-based rainfall observations are sparse or unavailable.

3.8. Implications for water resource modelling

The results demonstrate that PERSIANN-CCS precipitation can be effectively used as input for event-based rainfall–runoff modelling with HEC-HMS in the Nfifikh watershed. Although the simulation accuracy varies among flood events, the satellite product provides reliable streamflow simulations and represents a valuable source of precipitation information where rain-gauge observations are limited or unavailable.

From an operational perspective, the calibrated HEC-HMS model can support flood forecasting and water resources management by providing streamflow simulations in data-scarce environments. Furthermore, the simulated hydrographs can be directly used as upstream boundary conditions for hydraulic models, facilitating flood inundation mapping and flood hazard assessment. This modelling framework therefore provides a practical basis for improving flood risk management and supporting decision-making in the Nfifikh watershed, as well as in other semi-arid Moroccan catchments with similar hydrological characteristics.

Future work should evaluate the proposed methodology over longer observation periods, extend its application to larger catchments, and compare the performance of PERSIANN-CCS with other satellite precipitation products. Such investigations would provide a broader assessment of the applicability of satellite precipitation datasets for hydrological and hydraulic modelling under different climatic and physiographic conditions.

3.9. Limitations of the study

Like any hydrological modelling study, the present work has some limitations that should be acknowledged. Although precipitation observations from four rain-gauge stations were used to estimate basin-average rainfall through the Thiessen polygon method, the calibration and validation of the HEC-HMS model relied on discharge records from a single hydrometric station, Feddan Taba. Consequently, model performance could be assessed at the watershed outlet, but its ability to reproduce streamflow variations at other locations within the watershed could not be independently evaluated. Additional streamflow observations would help provide a more comprehensive assessment of the spatial representation of the simulated hydrological response.

Another limitation is that the analysis focused exclusively on the PERSIANN-CCS precipitation product. Although the results showed that this product could provide satisfactory hydrological simulations for several of the selected events, other widely used satellite precipitation products, such as GPM-IMERG, CHIRPS, and TRMM 3B42, were not evaluated within the same modelling framework. Consequently, the present study does not establish the relative performance of PERSIANN-CCS compared with other satellite products. Future research could include a multi-product comparison to provide a broader assessment of satellite precipitation inputs for hydrological modelling in Moroccan watersheds.

Finally, the proposed modelling framework was evaluated using nine flood events from a single watershed, with six events used for calibration and three independent events used for validation. Although this selection allowed the model to be evaluated under different rainfall and hydrological conditions, the results do not necessarily represent the full range of flood responses that may occur in the watershed. Applying the same framework to additional flood events and watersheds with different climatic and physiographic characteristics would help further assess the robustness and transferability of the approach.

Conclusion

This study evaluated the performance of the HEC-HMS model for streamflow simulation in the Oued Nfifikh watershed using both observed rainfall and corrected PERSIANN-CCS satellite precipitation. The results showed that the model was able to satisfactorily reproduce the hydrological response of the watershed following a manual

calibration procedure refined through automatic calibration. The comparison between the two rainfall data sources indicated that model performance depended on the characteristics of each rainfall event, with neither dataset consistently outperforming the other. Overall, the simulations driven by corrected PERSIANN-CCS rainfall produced results comparable to those obtained using observed rainfall, highlighting the potential of this satellite precipitation product for hydrological applications in semi-arid watersheds.

Beyond the hydrological evaluation, this study provides a methodological framework for the use of corrected satellite precipitation data in flood forecasting and water resources management. The simulated hydrographs can be used as input for hydraulic models such as HEC-RAS to support flood hazard mapping. Future research should extend this approach to other watersheds, longer observation periods, and additional satellite precipitation products in order to further validate the findings and broaden the applicability of this methodology.

REFERENCE

1. Agence du Bassin Hydraulique du Bouregreg et de la Chaouia. (2012). Plan directeur d'aménagement intégré des ressources en eau du bassin du Bouregreg et de la Chaouia : Note de synthèse. https://abhbc.com/sites/default/files/2020-09/Synthese-PDAIRE-%20francais.pdf

2. Barnett, T. P., Adam, J. C., & Lettenmaier, D. P. (2005). Potential impacts of a warming climate on water availability in snow-dominated regions. *Nature, 438*(7066), 303–309. https://doi.org/10.1038/nature04141

3. Beck, H. E., van Dijk, A. I. J. M., Levizzani, V., Schellekens, J., Miralles, D. G., Martens, B., & de Roo, A. (2017). Global evaluation of SM2RAIN precipitation estimates. *Geophysical Research Letters, 44*(8), 3875–3882. https://doi.org/10.1002/2017GL072817

4. Bedada, B. A. (2025). Comparative rainfall-runoff hydrological modeling over central Ethiopia using ground observation and global satellite precipitation products: Remote sensing support for water resource management. *Discover Applied Sciences, 7*, Article 826. https://doi.org/10.1007/s42452-025-07448-6

5. Beven, K. D. (2012). *Rainfall–runoff modelling: The primer* (2nd ed.). Wiley-Blackwell.

6. Chai, T., & Draxler, R. R. (2014). Root mean square error (RMSE) or mean absolute error (MAE)? Arguments against avoiding RMSE in the literature. *Geoscientific Model Development, 7*, 1247–1250. https://doi.org/10.5194/gmd-7-1247-2014

7. Chow, V. T., Maidment, D. R., & Mays, L. W. (1988). *Applied hydrology*. McGraw-Hill.

8. Clark, C. O. (1945). Storage and the unit hydrograph. *Transactions of the American Society of Civil Engineers, 110*(1), 1419–1446. https://doi.org/10.1061/TACEAT.0005800

9. Dahal, D., & Kodima, T. (2025). Evaluating the performance of hydrological models for flood discharge simulation in the Wangchu River Basin, Bhutan. *Hydrology, 12*(3), Article 51. https://doi.org/10.3390/hydrology12030051

10. El Martili, I., Barkouki, K., Ahattab, J., Serhir, N., & Bensallam, S. (2025). Evaluation and improvement of PERSIANN-CCS precipitation data at multiple temporal scales in the Bouregreg–Chaouia Basin (Morocco). *Journal of Water and Climate Change, 16*(5), 1804–1830. https://doi.org/10.2166/wcc.2025.716

11. Elhakeem, M., & Papanicolaou, A. N. (2009). Estimation of the runoff curve number via direct rainfall simulator measurements in the State of Iowa, USA. *Hydrological Sciences Journal, 54*(5), 961–973. https://doi.org/10.1623/hysj.54.5.961

12. Farki, K., Zahour, G., Zerhouni, Y., & Wafa, H. (2012). Contribution à la compréhension de l'évolution sédimentaire et tectono-volcanique de la série triasico-liasique de l'Oued N'Fifikh (Meseta côtière, Maroc). *Annales de la Société Géologique du Nord, 19*, 145–156. https://doi.org/10.54563/asgn.1479

13. Gebregiorgis, A. S., & Hossain, F. (2013). Understanding the dependence of satellite rainfall uncertainty on topography and climate for hydrologic model simulation. *IEEE Transactions on Geoscience and Remote Sensing, 51*(1), 704–718. https://doi.org/10.1109/TGRS.2012.2196282

14. Gebregiorgis, A. S., & Hossain, F. (2015). How effective is the satellite-based rainfall estimation for hydrologic prediction over data-scarce regions? *Journal of Hydrometeorology, 16*(4), 1695–1709.

15. Gupta, H. V., Sorooshian, S., & Yapo, P. O. (1999). Status of automatic calibration for hydrologic models: Comparison with multilevel expert calibration. *Journal of Hydrologic Engineering, 4*(2), 135–143. https://doi.org/10.1061/(ASCE)1084-0699(1999)4:2(135)

16. Gupta, H. V., Kling, H., Yilmaz, K. K., & Martinez, G. F. (2009). Decomposition of the mean squared error and NSE performance criteria: Implications for improving hydrological modelling. *Journal of Hydrology, 377*(1–2), 80–91. https://doi.org/10.1016/j.jhydrol.2009.08.003

17. Halwatura, D., & Najim, M. M. M. (2013). Application of the HEC-HMS model for runoff simulation in a tropical catchment. *Environmental Modelling & Software, 46*, 155–162. https://doi.org/10.1016/j.envsoft.2013.03.006

18. Hawkins, R. H., Ward, T. J., Woodward, D. E., & Van Mullem, J. A. (Eds.). (2009). *Curve number hydrology: State of the practice*. American Society of Civil Engineers.

19. Hong, Y., Hsu, K.-L., Sorooshian, S., & Gao, X. (2004). Precipitation estimation from remotely sensed imagery using an artificial neural network cloud classification system. *Journal of Applied Meteorology, 43*(12), 1834–1853. https://doi.org/10.1175/JAM2173.1

20. Hydrologic Engineering Center. (2023). *HEC-HMS technical reference manual*. U.S. Army Corps of Engineers. https://www.hec.usace.army.mil/software/hec-hms/documentation/HEC-HMS_Technical_Reference_Manual-20231106.pdf

21. Legates, D. R., & McCabe, G. D. (1999). Evaluating the use of "goodness-of-fit" measures in hydrologic and hydroclimatic model validation. *Water Resources Research, 35*(1), 233–241. https://doi.org/10.1029/1998WR900018

22. Maidment, D. R. (Ed.). (1993). *Handbook of hydrology*. McGraw-Hill.

23. Merbouh, C., Kabriti, M., Nahli, A., Rihane, A., & Iounes, N. (2023). Physicochemical characterization and metallic contamination of the waters of Oued Nfifikh (Morocco). *Ecological Engineering & Environmental Technology, 24*(1), 1–11. https://doi.org/10.12912/27197050/154911

24. Mishra, S. K., & Singh, V. P. (2003). *Soil Conservation Service curve number (SCS-CN) methodology*. Springer.

25. Moriasi, D. N., Arnold, J. G., Van Liew, M. W., Bingner, R. L., Harmel, R. D., & Veith, T. L. (2007). Model evaluation guidelines for systematic quantification of accuracy in watershed simulations. *Transactions of the ASABE, 50*(3), 885–900. https://doi.org/10.13031/2013.23153

26. Nash, J. E., & Sutcliffe, J. V. (1970). River flow forecasting through conceptual models part I—A discussion of principles. *Journal of Hydrology, 10*(3), 282–290. https://doi.org/10.1016/0022-1694(70)90255-6

27. Nguyen, P., Shearer, E. J., Tran, H., Ombadi, M., Hayatbini, N., Palacios, T., Huynh, P., Braithwaite, D., Updegraff, G., Hsu, K., Kuligowski, B., Logan, W. S., & Sorooshian, S. (2019). The CHRS Data Portal, an easily accessible public repository for PERSIANN global satellite precipitation data. *Scientific Data, 6*, Article 180296. https://doi.org/10.1038/sdata.2018.296

28. Ponce, V. M., & Hawkins, R. H. (1996). Runoff curve number: Has it reached maturity? *Journal of Hydrologic Engineering, 1*(1), 11–19. https://doi.org/10.1061/(ASCE)1084-0699(1996)1:1(11)

29. Refsgaard, J. C. (1997). Parameterisation, calibration and validation of distributed hydrological models. *Journal of Hydrology, 198*(1–4), 69–97. https://doi.org/10.1016/S0022-1694(96)03329-X

30. Ross, C. W., Prihodko, L., Anchang, J., Kumar, S., Ji, W., & Hanan, N. P. (2018). Global hydrologic soil groups (HYSOGs250m) for curve number–based runoff modeling. *Scientific Data, 5*, Article 180091. https://doi.org/10.1038/sdata.2018.91

31. Saouabe, T., El Khalki, E. M., Saidi, M. E. M., Najmi, A., Hadri, A., Rachidi, S., Jadoud, M., & Tramblay, Y. (2020). Evaluation of the GPM-IMERG precipitation product for flood modeling in a semi-arid mountainous basin in Morocco. *Water, 12*(9), Article 2516. https://doi.org/10.3390/w12092516

32. Tang, G., Ma, Y., Long, D., Zhong, L., & Hong, Y. (2013). Comparing satellite rainfall products with gauge observations in a mountainous area of China. *Journal of Hydrology, 497*, 120–131. https://doi.org/10.1016/j.jhydrol.2013.05.036

33. Tramblay, Y., Thiemig, V., Dezetter, A., & Hanich, L. (2016). Evaluation of satellite-based rainfall products for hydrological modelling in Morocco. *Hydrological Sciences Journal, 61*(14), 2509–2519. https://doi.org/10.1080/02626667.2016.1154149

34. U.S. Department of Agriculture, Soil Conservation Service. (1986). *Urban hydrology for small watersheds* (Technical Release 55, 2nd ed.).

35. U.S. Soil Conservation Service. (1972). *National engineering handbook: Section 4—Hydrology*. U.S. Department of Agriculture.

36. Willmott, C. J., & Matsuura, K. (2005). Advantages of the mean absolute error (MAE) over the root mean square error (RMSE) in assessing average model performance. *Climate Research, 30*, 79–82. https://doi.org/10.3354/cr030079

37. Yusop, Z., Chan, C. H., & Katimon, A. (2007). Runoff characteristics and application of HEC-HMS for modelling stormflow hydrograph in an oil palm catchment. *Water Science and Technology, 56*(8), 41–48. https://doi.org/10.2166/wst.2007.690